Performance of Quinoxalinone Derivatives as a Potential Efficient Inhibitor of Ordinary Steel Corrosion in 1 M Hydrochloric Acid: DFT Calculations

A. Benallal[1], M. Galai[2], F. Benhiba[2], N. M'hanni[2], Rachid Hsissou[3]*, S. Ibn Ahmed[1], M. Ebn Touhami[2], H. Oudda[2], S. Boukhris[1] and A. Souizi[1]

[1] Laboratory of Organic Chemistry, Catalysis and Environment, Department of Chemistry, Faculty of Sciences, Ibn Tofail University, P. O. Box 242, 14000 Kenitra, Morocco
[2] Laboratory of Advanced Materials and Process Engineering, Faculty of Sciences, Ibn Tofail University, P. O. Box 242, 14000 Kenitra, Morocco
[3]Laboratory of Organic Chemistry, Bioorganic and Environment, Chemistry Department, Faculty of Sciences, Chouaib Doukkali University, El Jadida, Morocco
Corresponding authors: r.hsissou@gmail.com, galaimouhsine@gmail.com

Received 02/02/2022; accepted 05/05/2022
https://doi.org/10.4152/pea.2023410604

Abstract
Two quinoxalinone derivatives, namely 3- (p-tolyl)-3.4-dihydroquinoxalin-2-(1H)-one (Q1) and 3-(4-chlorophenyl)-4-methyl-3.4-dihydroquinoxalin-2-(1H)-one (Q2), were used and investigated as potential corrosion inhibitors for OS in a 1 M HCl solution, at C from 10^{-6} to 10^{-3} M, using PDP, EIS measurements and GQCD calculations. EIS results indicate that Q1 and Q2 IE(%) increased with higher C and reached maximum values of 86.2 and 92.5%, at 10^{-3} M, respectively. The inhibitors adsorption mechanism onto the OS surface was found to obey the Langmuir's adsorption isotherm model. PDP data displayed that Q1 and Q2 acted as mixed inhibitors, predominantly of the cathodic type. The theoretical results showed that the obtained parameters were in good agreement with the experimental data. Q2 compound had better IE(%), due to the inductive effect of CH3 electro-donor group in dihydroquinoxaline position.

Keywords: corrosion inhibition, GQCD calculations, HCl, OS, PDP/EIS and Quinoxalinone derivatives.

Introduction •

Corrosion results from the environment chemical or electrochemical action on metals and alloys. Corrosion inhibitors are substances that are added to aggressive environments, such as acid pickling, chemical cleaning and oil wells acidification processes, since they can significantly reduce the attack rate of metals and alloys, by decreasing corrosion processes [1-4]. In spite of this, large amounts of steel are destroyed in acidic media, especially HCl, due to corrosion [5, 6]. Acidic solutions are more widely used in industrial fields (fertilizers manufacture, pickling and metal scaling) [7-9]. In a large number of articles, reviews and books, the use of heterocyclic

• The abbreviations and symbols definition lists are in pages 459-460.

compounds as corrosion inhibitors of metals in acidic media has been investigated [10-12]. Among the most emblematic works, there is the review published by Schmitt, in 1984, “Application of inhibitors for acid media” [13]. Thus, we will briefly describe recent works that deal, in particular, with the field of Fe and steel acidic corrosion protection by heterocyclic compounds containing several heteroatoms [14-17]. Steel corrosion in 1 M HCl has been studied by Elayyachy et al. [18]. Galai et al. have shown that the increase in N atoms electron density enhances IE(%) [1], while heterocyclic compounds containing N heteroatoms, such as pyridine, quinoline and various amines, have obtained good IE(%) in acidic media [19, 20]. H atom substitution by pyridine increases considerably its inhibitory action [21]. The authors evaluated the studied polymer IE(%), by using WL and electrochemical techniques, namely, PDP and EIS [22-24]. Due to quinoxalines (e.g. indeno-1-one [2, 3-b] quinoxaline, acenaphtho [1,2-b] quinoxaline, ethyl 2- (4-(2-ethoxy-2-oxoethyl)-2-p-tolylquinoxalin-1 (4H)-yl) acetate and 1- [4-acetyl-2- (4-chlorophenyl) quinoxalin-1(4H)-yl]acetone) excellent mechanical, thermal, viscosimetric and rheological properties[25-28], they have shown to be good inhibitors against acidic corrosion [20, 29-31]. Theoretical studies have been widely used to explain corrosion inhibition mechanism, interpret the experimental results, and also find a correlation between the organic compounds molecular structure and their IE(%). Global quantum chemical descriptors of the studied inhibitor molecules, such as HOMO, LUMO and μ, have been researched [32-40].

In the present work, Q1 and Q2 have been investigated as potential corrosion inhibitors for OS in a 1 M HCl medium, using electrochemical studies and theoretical calculations. Further, activation kinetic parameters, such as E_a, $\Delta H°$, $\Delta S°$ and $\Delta G°$, have been calculated and thoroughly discussed. The geometry optimization of the studied molecules and the parameters calculation were carried out using DFT method level, at 6-31G(d,p) basis set.

Materials and methods

OS used

OS chemical composition (% by wt.) is shown in Table 1.

Table 1. OS chemical composition.

Element	C	Si	Mn	Cr	Mo	Ni	Al	Cu	V	W	Fe
Mass(%)	0.11	0.24	0.47	0.12	0.02	0.1	0.03	0.14	<0.003	0.06	rest

The OS surface was a rectangle of 1 cm^2, which was prepared, before immersion, by polishing it with an abrasive paper up to a grain size of 2000. It was rinsed with distilled water and acetone, and dried with hot air. The corrosive medium was a 1 M HCl solution, prepared from the commercial solution (37%), using bi-distilled water. The C range used for the two tested inhibitors was from 10^{-6} to 10^{-3} M, which was determined after studying their solubility in the corrosive medium.

Used inhibitors

Quinoxalinone derivatives compounds were synthesized, as characterized by Lalami et al. [41], and their structures are listed in Table 2.

Table 2. Structures, masses and molecular formulas of the studied quinoxalinone derivatives.

Quinoxalinone derivatives	Abbreviation	Molecular structures	Molecular weight and chemical formula
3-(p-tolyl)-3,4-dihydroquinoxalin-2(1H)-one	Q1	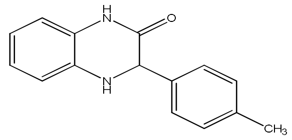	238.28 $C_{15}H_{14}N_2O$
3-(4-chlorophenyl)-4-methyl-3,4-dihydroquinoxalin-2(1H)-one	Q2	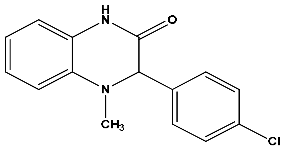	272.73 $C_{15}H_{13}ClN_2O$

Electrochemical measurements

The electrochemical experiments were carried out in a conditioned cell equipped with a conventional three-electrode arrangement: OS as WE, Pt as AE and Ag/AgCl as RE. Electrochemical methods for the study of corrosion can be classified into two main groups: the so-called stationary (classical) and non-stationary (transient) methods. In the first one, the intensity-E curves are obtained in a PDP mode, where the E applied to the sample varies continuously, with a SR of 1 mV/S^{-1}. The measurements were made by a PGZ100 Potentiostat-Galvanostat, associated with Voltamaster 4 software. Before the curves were drawn, the WE was maintained at its E, for 30 min. EIS measurements were made under the same conditions as those of the PDP plotting, at the frequency interval from 100 to 10 KHz.

DFT calculations

Optimization of the quinoxalinones compounds geometric structure was performed by the DFT method, with the non-local Lee-Yang-Parr correlation function (B3LYP), at 6-31G (d,p) basis set, using 09W Gaussian software [42]. The various GQCD parameters, such as χ, Pi and ΔE, are expressed by the following relations [43-46]:

$$\Delta E = E_{LUMO} - E_{HOMO} \quad (1)$$

$$Pi = -E_{HOMO} \quad (2)$$

$$A = -E_{LUMO} \quad (3)$$

$$\chi = \frac{Pi + A}{2} \quad (4)$$

η and σ are given by the following equations [47]:

$$\eta = \frac{Pi - A}{2} \quad (5)$$

$$\sigma = \frac{1}{\eta} = -\frac{2}{E_{HOMO} - E_{LUMO}} \quad (6)$$

ω was introduced by Parr [48, 49], and it is given by:

$$\omega = \frac{\mu^2}{2\eta} \quad (7)$$

This index measures the propensity of chemical species to accept electrons. A more reactive nucleophilic is characterized by μ and ω lower values; conversely, a good electrophile is characterized by μ and ω greater values. ΔN was calculated as follows [50]:

$$\Delta N = \frac{\chi_{Fe} - \chi_{inh}}{2\left(\eta_{Fe} + \eta_{inh}\right)} \qquad (8)$$

where χ_{Fe} and χ_{inh} represent Fe absolute χ and the inhibitor molecule, respectively; η_{Fe} and η_{inh} denote Fe absolute η and the inhibitor molecule, respectively; and $\chi_{Fe} = 7.0$ eV and $\eta_{Fe} = 0$ theoretical values were used to calculate ΔN [49].

Results and discussion

EIS analysis

In order to understand OS corrosion mechanisms, after 30 min of immersion in 1 M HCl, at 303 K, EIS diagrams obtained at E_{corr}, without and with Q1 and Q2, in different C, are shown in Figs. 1 and 2.

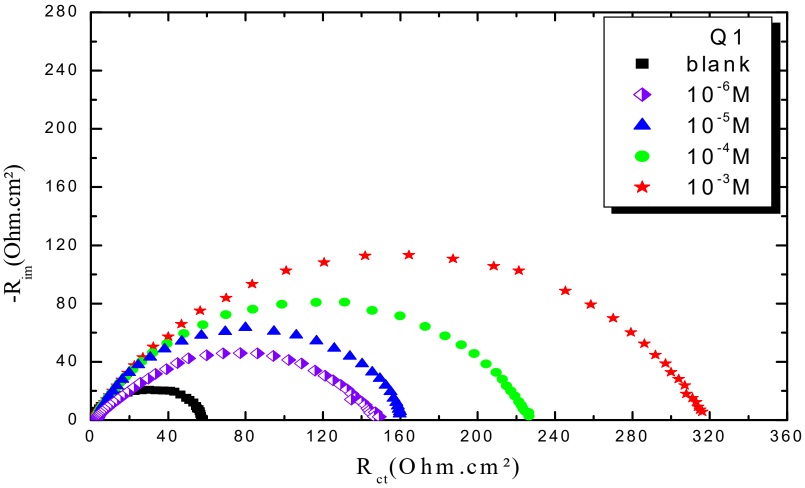

Figure 1. Nyquist diagram for OS in 1 M HCl, without and with Q1, in different concentrations.

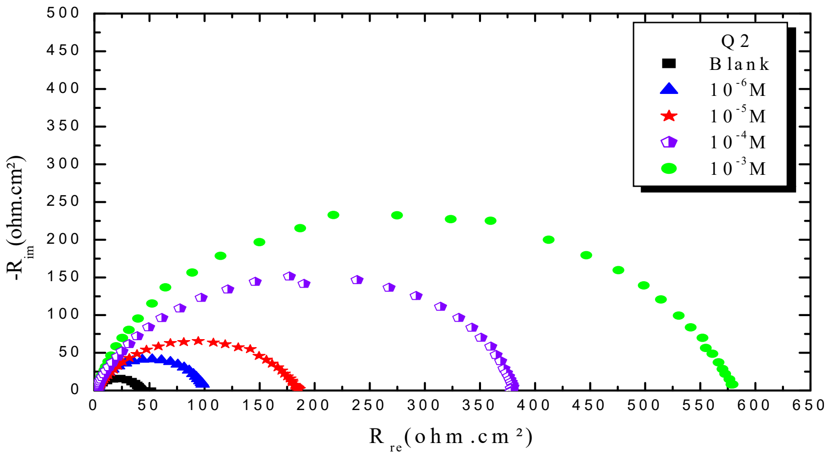

Figure 2. Nyquist diagram for OS in 1 M HCl, with and without Q2, in different concentrations.

From the analysis of Figs. 1 and 2, we note that there is a large increase in the loop, in Q1 and Q2 presence and, consequently, an increase in R_{ct}, which is inversely proportional to CR. Corrosion IE(%) and OS C_{dl} were calculated by the following equations [51-54]:

$$C_{dl}=\frac{1}{2\pi.Rct.f_{max}} \quad (9)$$

$$\eta\ \% = \frac{R_{ct}^{i} - R_{ct}^{\circ}}{R_{ct}^{i}} \times 100 \quad (10)$$

R_{ct}^{i} and R_{ct}° are values without and with the inhibitor, respectively. C_{dl} values are also expressed by the Helmholtz relation [55].

$$C_{dl} = \frac{\varepsilon^{\circ}\varepsilon}{\delta} S \quad (11)$$

where δ is the double layer capacity thickness, S is the OS electrode surface, and ε° and ε are vacuum and solution dielectric constants, respectively.
The electrochemical parameters associated with the impedance diagrams are recorded in Table 3.

Table 3. EIS parameters of OS in 1 M HCl without and with studied inhibitors, and their corrosion efficiencies IE(%) .

Inhibitors	Conc (M)	R_{ct} (ohm/cm²)	C_{dl} (µF/cm²)	IE(%)
Blank HCl	1	44	294	-
Q1	10^{-6}	148	296	72.2
	10^{-5}	161	227	73.0
	10^{-4}	225	200	80.5
	10^{-3}	319	133	86.2
Q2	10^{-6}	99	266	55.5
	10^{-5}	189	183	77.0
	10^{-4}	380	93	88.5
	10^{-3}	579	51	92.5

Table 3 indicates that P_r increased with higher C of the studied inhibitors. Further, Q1 and Q2 IE(%), at inhibitors optimal C of 10^{-3} M, reached the maximum values of 86.2 and 92.5%, respectively. C_{dl} was inversely proportional to R_{ct}. C_{dl} values calculated in the 1 M HCl medium without inhibitors were lower than of those with Q1 and Q2. This decreases can be attributed to the organic molecules adsorption onto the metallic surface [56, 57]. From these observations, it can be said that Q2 adsorption performance onto the metallic surface was higher than that of Q1.
The equivalent electrical circuit used to output the electrochemical parameters is shown in Fig. 3.

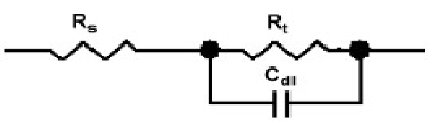

Figure 3. Equivalent electrical circuit of inhibitors/OS interface in 1 M HCl.

PDP investigation

Figs. 4 and 5 show the cathodic and anodic polarization curves of OS in 1 M HCl without Q1 and Q2 and with them in different C, at 298 K. The electrochemical parameters taken from these curves are grouped in Table 3. Figs. 4 and 5 show that the increases in C of the tested inhibitors led to a shift in I_{corr}, in the two anodic and cathodic domains, to lower values.

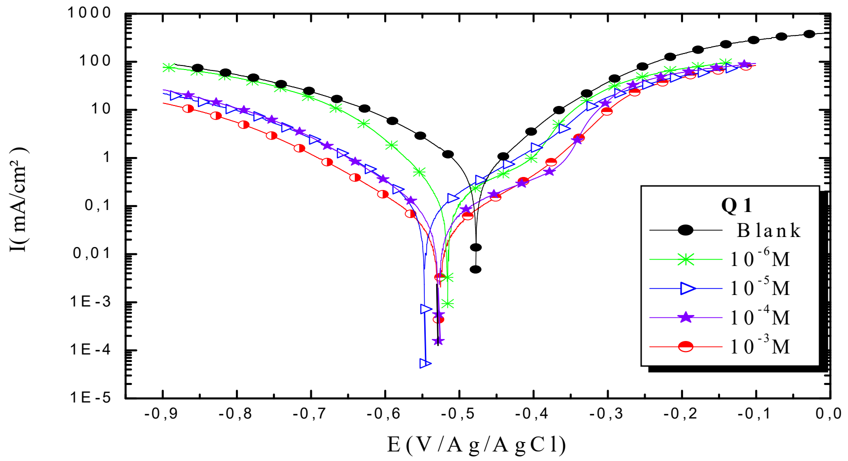

Figure 4. PDP of OS in 1 M HCl without and with Q1 at different concentrations, at 298 K.

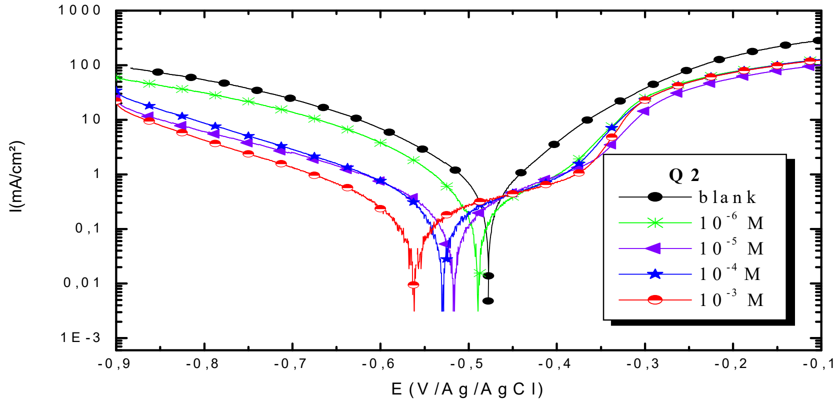

Figure 5. PDP of OS in 1 M HCl without and with Q2 in different concentration, at 298 K.

The cathodic slope is in the form of Tafel line, for the entire range of examined E, indicating that H reduction on the OS surface took place through a pure activation mechanism [58-60].

IE(%) was calculated by the following equation:

$$\eta_{Tafel}\% = \frac{I^{\circ}_{corr} - I^{i}_{corr}}{I^{\circ}_{corr}} \times 100 \qquad (12)$$

The electrochemical parameters determined from the polarization curves, such as E_{corr}, β_c, i_{corr} and IE(%), are grouped in Table 4.

Table 4. IE(%) and electrochemical parameters obtained from the curves of OS in 1 M HCl without and with inhibitors at different concentrations.

Inhibitors	C (M)	E_{corr} (mV/Ag/Agcl)	i_{corr} (µA/cm²)	$β_c$ (mV/dec^{-1})	IE(%)
Blank HCl	1	478	470	240	-
Q1	10^{-6}	556	140	194	70.2
	10^{-5}	530	129	111	72.5
	10^{-4}	520	92	103	80.5
	10^{-3}	491	61	99	87.1
Q2	10^{-6}	530	194	177	58.0
	10^{-5}	531	104	156	78.1
	10^{-4}	550	52	121	89.0
	10^{-3}	516	30	100	93.6

From the analysis of Table 3, we observed that, for all Q1 and Q2 C, i_{corr} decreased with higher inhibitor C and, consequently, IE% increased, reaching a maximum value of 87.1 and 93.6%, respectively. In general, this behavior is due to the active sites blocking by the formation of a protective layer on the OS surface.

The different C of the studied inhibitors slightly modified $β_c$ values, with respect to the blank HCl.

Thus, these compounds are mixed inhibitors, predominantly cathodic, because there was a displacement in the E_{corr} values, in both cathodic and anodic domains, with Q1 and Q2 different C in 1 M HCl. This maximum displacement was 78 mV/Ag/AgCl for Q1. $β_c$ and $β_a$ were extensively changed by Q1 and Q2. This modification indicates that the organic compounds derivatives, which were elaborated as potential inhibitors, were adsorbed onto the OS surface, by blocking the active centers through the chemical bonds.

Cathodic and anodic reactions for OS substrates were inhibited by Q1 and Q2. PDP results confirmed the data obtained by EIS measurements.

T effect

T effect on Q1 and Q2 IE(%) for OS corrosion in a 1 M HCl solution without and with them, in a C of 10^{-3} M, at a range from 298 to 318 K, was obtained by PDP measurements. Table 5 lists all the electrochemical parameters, as a function of the different T.

Table 5. PDP parameters of OS in 1 M HCl without and with Q1 and Q2 (10^{-3}M), at different T.

Inhibitors	T (K)	$-E_{corr}$ (mv/Ag/Agcl)	i_{corr} (µA/cm²)	IE(%)
Blank HCl	298	498	470	-
	308	491	1200	-
	318	475	1450	-
	328	465	2500	-
Q1	298	491	61	87.1
	308	478	210	82.5
	318	456	285	80.2
	328	503	533	79.0
Q2	298	526	30	93.6
	308	493	132	89.0
	318	491	201	86.1
	328	490	410	84.0

IE(%) underwent a decrease, while CR increased with higher T, in the absence of Q1 and Q2 and in their presence (10^{-3} M) .
Activation kinetic parameters, such as E_a, ΔH° and ΔS°, were calculated. E_a (kJ/mol^{-1}) relative to the corrosion process was calculated from Arrhenius equation:

$$k = E_a^{-E/RT} \tag{13}$$

where R is the perfect gas constant and T is absolute.
Fig. 6 shows the i_{corr} logarithm variations, as a function of T inverse.

$$\ln(i_{corr}) = f\,(1/t) \tag{14}$$

where ln is the natural logarithm, f is the frequency and t is the time period.

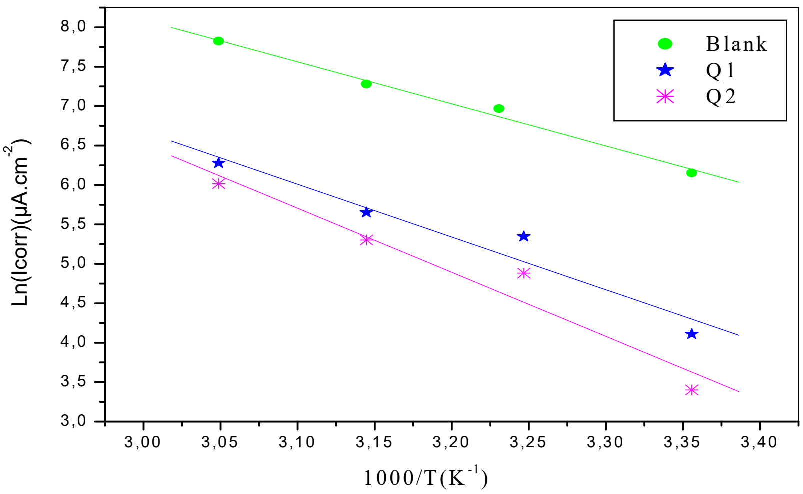

Figure 6. Arrhenius lines calculated from PDP for OS in 1 M HCl without and with Q1 and Q2 inhibitors.

The i_{corr} logarithm variations enabled to calculate E_a values from the slope of each one of the obtained straight lines. E_a values are listed in Table 6, which shows that this parameter, in HCl without Q1 and Q2 is higher than of that with them. This result is interpreted as an indication of an electrostatic character of the inhibitors adsorption. It can be said that the studied inhibitors were adsorbed onto the steel surface by forming physical bonds (physisorption) [6].
Another formulation of the Arrhenius equation is [61]:

$$I_{corr} = \frac{RT}{Nh}\exp\left(\frac{\Delta S_a^{\circ}}{R}\right)\exp\left(\frac{\Delta H_a^{\circ}}{RT}\right) \tag{15}$$

where h is the Plank constant and N is the Avogadro number.
Ln(i_{corr}/T) variation, as function of T inverse, is a straight line (Fig. 7), with a slope of 1000/R and an ordinate at the origin equal to (LnR/Nh + 1000/ R). Fig. 7 shows that the lines are almost straight, and that all R_2 values are close to 1. From the slopes and lines intersections, E_a, ΔH_a° and ΔS_a° values were computed and grouped in Table 6.

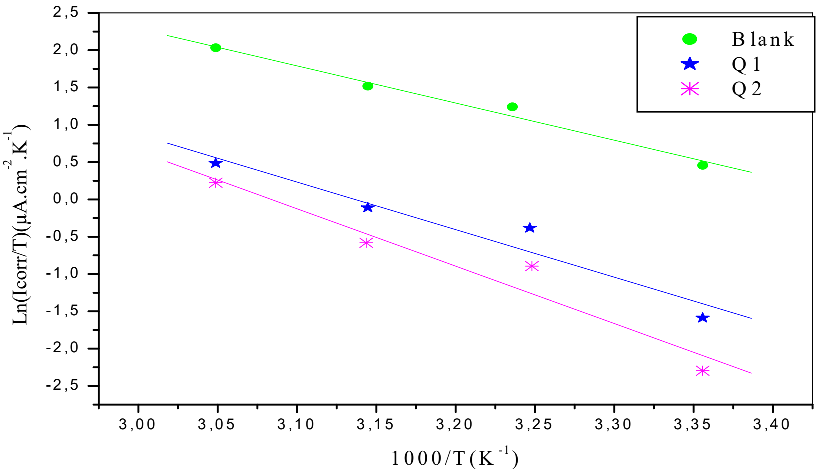

Figure 7. Ln (i_{corr}/T) as function of 1000/T for OS in 1 M HCl without and with Q1 and Q2 inhibitors.

The endothermic reactions positive values were expressed on the OS dissolution process. Indeed, the increase in ΔS_a° with Q1 and Q2 was 52.9 and 63.9 kJ/mol^{-1}, respectively, whereas in their absence it was 41.4 kJ./mol^{-1}, which corresponds to a decrease in the metal dissolution. The high and negative entropy values mean that there was an increase in disorder when the reactants were transformed into an activated Fe-molecule complex in the solution [1, 8, 35].

Table 6. E_a, ΔH_a° and ΔS_a° values without and with Q1 and Q2 inhibitors.

Inhibitors	**E_a (kJ/mol^{-1})**	**ΔH_a° (kJ/mol^{-1})**	**$-\Delta S_a^{\circ}$ (J/mol^{-1}/K^{-1})**
Blank HCl	44.3	41.4	54.3
Q1	55.7	52.9	31.2
Q2	67.5	63.9	0.2

Adsorption isotherm

The adsorption isotherm can give additional data on the compounds adsorption performance on the metal surface. θ values for different inhibitor C in a 1 M HCl solution were obtained according to the IE% ratio. There are several adsorption models, such as Langmuir's, Temkin's and Frumkin's isotherms, based on C_{inh}/θ. As a function of C_{inh}, we found that there were excellent experimental values for Q1 and Q2. For Langmuir's isotherm, its R^2 coefficient was close to 1, relative to those found in Temkin's and Frumkin's isotherms, as shown in Fig. 8 [45, 46, 62]. Therefore, experimental results obeyed the Langmuir's adsorption isotherm, where θ and C_{inh} are linked to each other via the equation:

$$\theta = \frac{K_{ads} C_{inh}}{1 + K_{\mathrm{ads}} C_{inh}} \tag{16}$$

The rearrangement gives:

$$\frac{C_{inh}}{\theta} = \frac{1}{K_{\text{ads}}} + C_{inh} \qquad (17)$$

K_{ads} can be calculated from the straight lines intersections.
Fig. 8 shows C_{inh}/θ variation, as a function of the inhibitor C, where the shown lines are close to one.

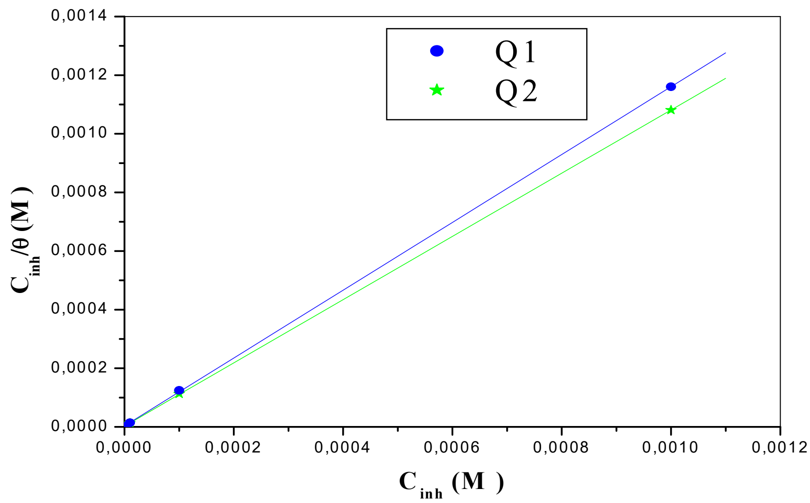

Figure 8. Langmuir's adsorption isotherm of OS in 1 M HCl with Q1 and Q2 inhibitors.

$\Delta G^{o}_{\text{ads}}$ is related to K_{ads} by relationship (16), and the corresponding results are listed in Table 7 [63].

$$\Delta G^{\text{o}}_{\text{ads}} = -RTLn\left(55.5K_{\text{ads}}\right) \qquad (18)$$

From Table 7, we find that K_{ads} values are high, indicating that Q1 and Q2 were readily adsorbed onto the OS surface [64]. In general, if $\Delta G^{o}_{\text{ads}}$ values are close to or greater than -20 kJ/mol, they are linked to electrostatic interactions; those which are close to -40 kJ/mol or lower involve the formation of chemical nature bonds between the inhibitor molecules and the metal surface. For $\Delta G^{o}_{\text{ads}}$ values in the range from -20 to -40 kJ/mol, the two phenomena apply at the same time [65]. However, these criteria remain insufficient in order to distinguish between the two phenomena (chemisorption and physisorption). The results in Table 8 indicate that the two inhibitors obeyed the order Q2> Q1. That is, Q2 adsorption performance onto the OS surface was higher than that of Q1, due to the existence of an electro-donor group on the N atom number four (N4) in the first compound.

Table 7. Thermodynamic parameters of Q1 and Q2 with different concentrations on the OS surface in 1 M HCl, at 298 K.

Inhibitors	**K_{ads}**	**R^2**	**$-\Delta G^{o}_{ads}$ (kJ/mol)**
Q1	289070.8	0.9999	41.1
Q2	384714.5	0.9999	41.8

DFT calculations

Quantum chemistry calculation was carried out by the DFT 6-31G (d, p) method, and compared with experimental results. During this study, we calculated chemical quantum parameters. Also, HOMO and LUMO optimized geometric structures and electron density distributions for these inhibitors are presented in Fig. 9. It is seen that HOMO and LUMO were distributed over Q1 and Q2 entire surfaces. This indicates that these molecules are rich in electrons.

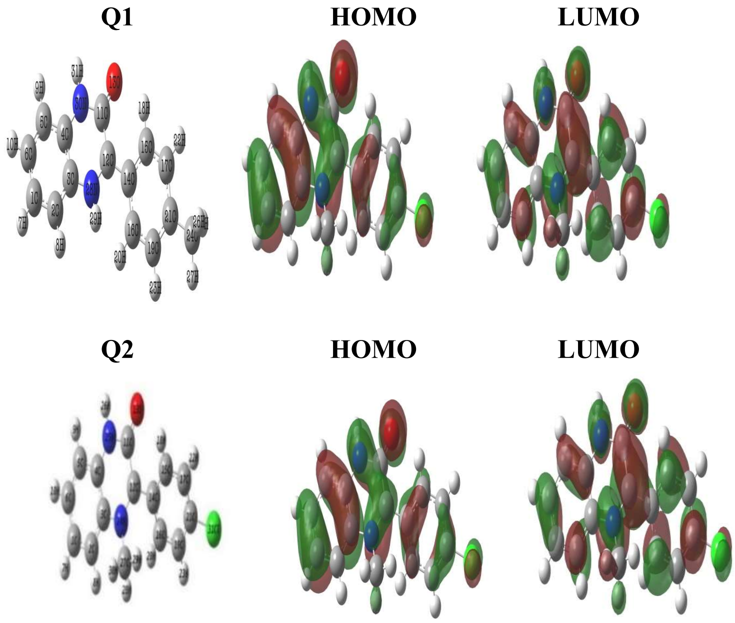

Figure 9. Optimized structures, HOMO and LUMO for studied molecules using DFT/B3LYP at 6-31G (d, p).

Mulliken atomic charges on the Q1 and Q2 atoms, the μ vector direction, and the contour and surface representation of the electrostatic E are presented in Figs. 10 and 11.

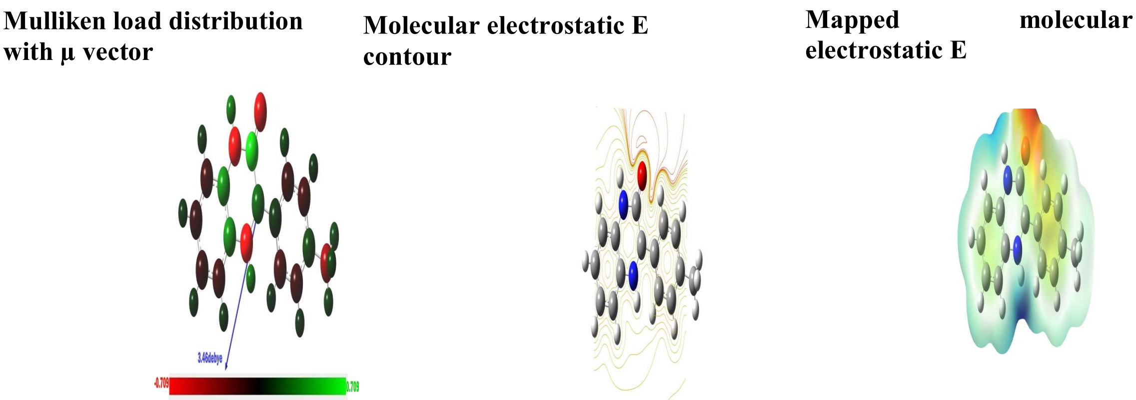

Figure 10. Mulliken charge and electrostatic properties for Q1 inhibitor.

From these figures, it is evident that the N, O and some C atoms for the two inhibitors carry negative charges. So, they are responsible for a nucleophilic attack towards the OS surface. The electrostatic E different values were given using red, yellow, green and blue. Red (electrophilic active regions) and blue (nucleophilic regions) represent MESP negative and positive parts and green depicts the zero region electrostatic E [66, 67]. Depending on the studied inhibitors ESP and MESP contour surfaces, the negative parts are electrophilic active regions mainly found on the O surface.

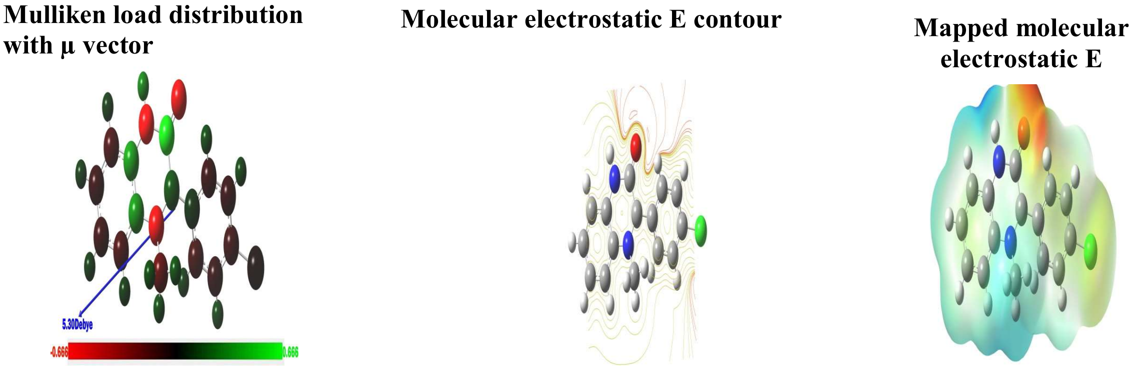

Figure 11. Mulliken charge and electrostatic properties for Q2 inhibitor.

E_{HOMO} indicates the molecule ability to give electrons to another empty molecular orbit; E_{LUMO} describes the ability of a compound to accept electrons. ΔE is the energy difference between E_{HOMO} and E_{LUMO}. The energy absorption between the inhibitors and the metal surface increases when ΔE decreases, i.e., the energy to remove an electron from the last occupied orbit will be low [68-70]. The corresponding results of the quantum parameters are presented in Table 8, from which we note that the ΔE values for Q1 and Q2 are 3.536 and 3.194<eV, respectively. Q2 had a weaker ΔE than that of Q1. This indicates that Q2 adsorption performance was greater than that of Q1, in the order: ΔE (Q1)>ΔE (Q2)

Consequently, η and σ are important properties for measuring molecular stability and reactivity. Q1 and Q2 IE(%) increased with higher chemical reactivity [71-75]. Q2 had good chemical reactivity with the metal surface, due to the increase in the σ value (0.626 eV^{-1}) and the decrease in η (1.597 eV), according to the following order: η (Q2)> η (Q1).

Q2 maximum µ value was 5.304 Debye, which shows that this is highly polarizable. So, Q2 is very reactive, which could be related to the µ-µ interaction between the inhibitor molecules and the metal surface [12, 76, 77].

Q2 had a minimum Pi of 5.545 eV, indicating that it is more effective. On the other hand, the IE(%) was higher with an increase in the inhibitor electron donor capacity to the metal surface. The transferred electrons displacement from the inhibitor to the metal surface occurred in the following order: ΔN = 0.955 (Q2) > ΔN = 0.872 (Q1).

Table 8 shows that Q2 had higher ω than that of Q1 (9.626 eV). It was found that this inhibitor acts as an electrophile (electron acceptor). Finally, Q2 total energy was equal to -1223.76 a.u, which indicates that it was favorably adsorbed through the active adsorption centers.

Table 8. Chemical quantum parameters for studied inhibitors (Q1 and Q2).

Parameter	Q1	Q2
E_{LUMO} (eV)	-2.147	-2.351
E_{HOMO} (eV)	-5.683	-5.545
ΔEgap (eV)	3.536	3.194
μ (debyes)	3.361	5.304
η (eV)	1.768	1.597
σ ($e.V^{-1}$)	0.565	0.626
Pi (e.V)	5.683	5.545
χ (eV)	3.915	3.948
A (eV)	2.147	2.351
ΔN (eV)	0.872	0.955
ω (eV)	9.133	9.626
TE (u.a)	-764.18	-1223.76

The theoretical study showed that quantum parameters were in agreement with experimental observations.

Conclusion

Two quinoxalinone derivatives were used to inhibit OS corrosion in a 1 M HCl medium. The study was carried out using various experimental and theoretical approaches. The results of this study are as follows:

- Q1 and Q2 inhibitors were effective inhibitors for OS corrosion.
- Those molecules were mixed inhibitors, of predominantly the cathodic type.
- EIS results displayed that the Nyquist diagrams had a single capacitive loop, indicating that the corrosion inhibition was controlled by R_{ct} process.
- T effect suggested that IE(%) decreased with higher T.
- The studied inhibitors adsorption onto the OS surface in a 1 M HCl solution obeyed Langmuir's adsorption isotherm.
- Theoretical approaches and experiments data were in good agreement.

Authors' contributions

A. Benallal: collected the data. **M. Galai**: performed the analysis. **F. Benhiba**: performed the analysis; wrote the paper. **N. M'hanni**: wrote the paper. **Rachid Hsissou**: wrote the paper. **S. Ibn Ahmed**: conceived and designed the analysis. **M. Ebn Touhami**: conceived and designed the analysis. **H. Oudda**: other contributions. **S. Boukhris**: contributed with data or analysis tools. **A. Souizi**: conceived and designed the analysis.

Abbreviations

AE: auxiliary electrode
C: concentration
C_{dl}: double layer capacity
CR: corrosion rate
DFT: density functional theory
E_a: activation energy
E: potential
E_{corr}: corrosion potential
EIS: electrochemical impedance spectroscopy

E_{HOMO}: energy of the highest occupied molecular orbital
E_{LUMO}: energy of the lowest unoccupied molecular orbital
GQCDs: global quantum chemical descriptors
HOMO: highest occupied molecular orbital
I_{corr}: corrosion current density
IE(%): corrosion inhibition efficiency
K_{ads}: equilibrium constant of adsorption
LUMO: lowest unoccupied molecular orbital
MESP: molecular electrostatic potential
OS: ordinary steel
Pi: ionization potential
PDP: potentiodynamic polarization
P_r: polarization resistance
R_2: regression coefficient
R_{ct}: charge transfer resistance
RE: reference electrode
SR: scan rate
T: temperature
WE: working electrode
WL: weight loss

Symbols definition
β_c: Tafel slope
ΔE_{gap}: gap energy
ΔG°: activation free enthalpy
ΔG°_{ads}: adsorption free energy
ΔH°: activation standard enthalpy
ΔS°: activation standard entropy
η: chemical hardness
μ: dipole moment
σ: chemical softness
θ: surface coverage rate values
ω: overall electrophile index
χ: electronegativity

References

[1] Galai M, Rbaa M, Ouakki M et al. Chemically functionalized 8-hydroxyquinoline derivatives as efficient corrosion inhibition for steel in 1.0 M HCl solution: Experimental and theoretical studies. Surf Interf. 2020;21:100695. https://doi.org/10.1016/j.surfin.2020.100695
[2] Rbaa M, Benhiba F, Hssisou R et al. Green synthesis of novel carbohydrate polymer chitosan oligosaccharide grafted on d-glucose derivative as bio-based corrosion inhibitor. J Mol Liq. 2021;322:114549. https://doi.org/10.1016/j.molliq.2020.11454977
[3] Hssisou R, Abbout S, Benhiba F et al. Insight into the corrosion inhibition of novel macromolecular epoxy resin as highly efficient inhibitor for carbon steel in acidic mediums: Synthesis, characterization, electrochemical

techniques, AFM/UV–Visible and computational investigations. J Mol Liq. 2021;337:116492. https://doi.org/10.1016/j.molliq.2021.116492

[4] Hssisou R, Abbout S, Safi Z et al. Synthesis and anticorrosive properties of epoxy polymer for CS in 1 M HCl solution: Electrochemical, AFM, DFT and MD simulations. Constr Build Mat. 2021;270:121454. https://doi.org/10.1016/j.conbuildmat.2020.121454

[5] Galai M, El Faydy M, El Kacimi Y et al. Synthesis, characterization and anti-corrosion properties of novel quinolinol on C-steel in a molar hydrochloric acid solution. Port Electrochim Acta. 2017;35:233-251. https://doi:10.4152/pea.201704233

[6] Benhiba F, Hsissou R, Benzekri Z et al. Nitro substituent effect on the electronic behavior and inhibitory performance of two quinoxaline derivatives in relation to the corrosion of mild steel in 1 M HCl. J Mol Liq. 2020;312:113367. https://doi.org/10.1016/j.molliq.2020.113367

[7] Rbaa M, Fardioui M, Verma C et al. 8-Hydroxyquinoline based chitosan derived carbohydrate polymer as biodegradable and sustainable acid corrosion inhibitor for mild steel: Experimental and computational analyses. Int J Bio Macromol. 2020;155:645-655. https://doi.org/10.1016/j.ijbiomac.2020.03.200

[8] Ouass A, Galai M, Ouakki M et al. Poly(sodium acrylate) and Poly(acrylic acid sodium) as an eco-friendly corrosion inhibitor of mild steel in normal hydrochloric acid: experimental, spectroscopic and theoretical approach. J Appl Electrochem. 2021. https://doi.org/10.1007/s10800-021-01556-y

[9] Kadiri L, Galai M, Ouakki M et al. *Coriandrum Sativum* L seeds extract as a novel green corrosion inhibitor for mild steel in 1.0 M hydrochloric and 0.5 M sulfuric solutions. Analyt Bioanalyt Chem. 2018;10:249-268.

[10] Hsissou R, Benhiba F, Echihi S et al. Performance of curing epoxy resin as potential anticorrosive coating for carbon steel in 3.5% NaCl medium: Combining experimental and computational approaches. Chem Phys Lett. 2021;783:139081. https://doi.org/10.1016/j.cplett.2021.139081

[11] Hsissou R, Benhiba F, Echihi S et al. New epoxy composite polymers as a potential anticorrosive coatings for carbon steel in 3.5% NaCl solution: Experimental and computational approaches. Chem Data Coll. 2021;31:100619. https://doi.org/10.1016/j.cdc.2020.100619

[12] Hsissou R. Review on epoxy polymers and its composites as a potential anticorrosive coatings for carbon steel in 3.5% NaCl solution: Computational approaches. J Mol Liq. 2021;336:116307. https://doi.org/10.1016/j.molliq.2021.116307

[13] Samide A, Bibicu I, Rogalski M et al. A study of the corrosion inhibition of carbon-steel in dilluted ammonia media using 2-mercapto-benzothiazol (MBT). Acta Chim Sloven. 2004;51:127-136.

[14] Hssissou R, Benzidia B, Hajjaji N et al. Elaboration, Electrochemical Investigation and morphological Study of the Coating Behavior of a New Polymeric Polyepoxide Architecture: Crosslinked and Hybrid Decaglycidyl of Phosphorus Penta methylene Dianiline on E24 Carbon Steel in 3.5% NaCl. Port Electrochim Acta. 2019;37:179-191. https://doi:10.4152/pea.201903179

[15] Hsissou R, Benzidia B, Hajjaji N et al. Elaboration and electrochemical studies of the coating behavior of a new pentafunctional epoxy polymer:

pentaglycidyl ether pentabisphenol A phosphorus on E24 carbon steel in 3.5% NaCl. J Chem Technol Metallur. 2018;3:898-905.
[16] Hsissou R, Benzidia B, Hajjaji N et al. Elaboration and electrochemical studies of the coating behavior of a new nanofunctional epoxy polymer on E24 steel in 3.5% NaCl. Port Electrochim Acta. 2018;36:259-270. https://doi:10.4152/pea.201804259
[17] Hsissou R, Bekhta A, Elharfi A et al. Theoretical and electrochemical studies of the coating behavior of a new epoxy polymer: hexaglycidyl ethylene of methylene dianiline (HGEMDA) on E24 steel in 3.5% NaCl. Port Electrochim Acta. 2018;36:101-117. https://doi:10.4152/pea.201802101
[18] Elayyachy M, Hammouti B, El Idrissi A et al. Adsorption and corrosion inhibition behavior of C38 steel by one derivative of quinoxaline in 1 M HCl. Port Electrochim Acta. 2011;29:57-68. https://doi:10.4152/pea.201101057
[19] Rbaa M, Benhiba F, Galai M et al. Synthesis and characterization of novel Cu (II) and Zn (II) complexes of 5-{[(2-Hydroxyethyl) sulfanyl] methyl}-8-hydroxyquinoline as effective acid corrosion inhibitor by experimental and computational testings. Chem Phys Lett. 2020;754:137771. https://doi.org/10.1016/j.cplett.2020.137771
[20] Rbaa M, Benhiba F, Dohare P et al. Synthesis of new epoxy glucose derivatives as a non-toxic corrosion inhibitors for carbon steel in molar HCl: Experimental, DFT and MD simulation. Chem Data Coll. 2020;27:100394. https://doi.org/10.1016/j.cdc.2020.100394
[21] Obot I, Obi-Egbedi N. Indeno-1-one [2, 3-b] quinoxaline as an effective inhibitor for the corrosion of mild steel in 0.5 M H_2SO_4 solution. Mat Chem Phys. 2010;122:325-328. doi.org/10.1016/j.matchemphys.2010.03.037
[22] Hsissou R, Dagdag O, Berradi M et al. Development rheological and anti-corrosion property of epoxy polymer and its composite. Heliyon. 2019;5:e02789. https://doi.org/10.1016/j.heliyon.2019.e02789
[23] Hsissou R, Dagdag O, Abbout S et al. Novel derivative epoxy resin TGETET as a corrosion inhibition of E24 carbon steel in 1.0 M HCl solution. Experimental and computational (DFT and MD simulations) methods. J Mol Liq. 2019;284:182-192. https://doi.org/10.1016/j.molliq.2019.03.180
[24] Hsissou R, Abbout S, Berisha A et al. Experimental, DFT and molecular dynamics simulation on the inhibition performance of the DGDCBA epoxy polymer against the corrosion of the E24 carbon steel in 1.0 M HCl solution. J Mol Struc. 2019;1182:340-351. https://doi.org/10.1016/j.molstruc.2018.12.030
[25] Hsissou R, Bekhta A, Elharfi A. Viscosimetric and rheological studies of a new trifunctional epoxy pre-polymer with noyan ethylene: Triglycidyl Ether of Ethylene of Bisphenol A (TGEEBA). J Mater Environ Sci. 2017;8:603-610.
[26] Hsissou R, El Bouchti M, Elharfi A. Elaboration and viscosimetric, viscoelastic and rheological studies of a new hexafunctional polyepoxide polymer: hexaglycidyl ethylene of methylene dianiline. J Mater Environ Sci. 2017;8:4349-4361.
[27] Bekhta A, Hsissou R, Elharfi A. Evaluation of mechanical compressive strength of cementitious matrix with 12% of IER formulated by modified polymer (NEPS) at different percentages. Sci Rep. 2020;10:1-8. doi.org/10.1038/s41598-020-59482-6

[28] El-Aouni N, Hsissou R, Azzaoui JE et al. Synthesis rheological and thermal studies of epoxy polymer and its composite. Chem Data Coll. 2020;30:100584. https://doi.org/10.1016/j.cdc.2020.100584
[29] Rbaa M, Oubihi A, Hajji H et al. Synthesis, bioinformatics and biological evaluation of novel pyridine based on 8-hydroxyquinoline derivatives as antibacterial agents: DFT, molecular docking and ADME/T studies. J Mol Struc. 2021;1244:130934. https://doi.org/10.1016/j.molstruc.2021.130934
[30] Rbaa M, Oubihi A, Anouar EH et al. Synthesis of new heterocyclic systems oxazino derivatives of 8-Hydroxyquinoline: Drug design and POM analyses of substituent effects on their potential antibacterial properties. Chem Data Coll. 2019;24:100306. https://doi.org/10.1016/j.cdc.2019.100306
[31] Rbaa M, Lgaz H, El Kacimi Y et al. Synthesis, characterization and corrosion inhibition studies of novel 8-hydroxyquinoline derivatives on the acidic corrosion of mild steel: Experimental and computational studies. Mat Disc. 2018;12:43-54. https://doi.org/10.1016/j.md.2018.11.003
[32] Bentiss F, Traisnel M, Lagrenee M. Influence of 2, 5-bis (4-dimethylaminophenyl)-1, 3, 4-thiadiazole on corrosion inhibition of mild steel in acidic media. J App Electrochemi. 2001;31:41-48. https://doi.org/10.1023/A:1004141309795
[33] El-Aouni N, Hsissou R, Safi Z et al. Performance of two new epoxy resins as potential corrosion inhibitors for carbon steel in 1 M HCl medium: combining experimental and computational approaches. Coll Surf A: Physicochem Eng Asp. 2021;626:127066. https://doi.org/10.1016/j.colsurfa.2021.127066
[34] Benhiba F, Serrar H, Hsissou R et al. Tetrahydropyrimido-Triazepine derivatives as anti-corrosion additives for acid corrosion: chemical, electrochemical, surface and theoretical studies. Chem Phys Lett. 2020;743:137181. https://doi.org/10.1016/j.cplett.2020.137181
[35] Benhiba F, Hsissou R, Benzekri Z et al. DFT/electronic scale, MD simulation and evaluation of 6-methyl-2-(p-tolyl)-1,4-dihydroquinoxaline as a potential corrosion inhibitor. J Mol Liq. 2021;335:116539. https://doi.org/10.1016/j.molliq.2021.116539
[36] Dagdag O, Hsissou R, El Harfi A et al. Epoxy resins and their zinc composites as novel anti-corrosive materials for copper in 3% sodium chloride solution: experimental and computational studies. J Mol Liq. 2020;315:113757. https://doi.org/10.1016/j.molliq.2020.113757
[37] Dagdag O, Hsissou R, El Harfi A et al. Development and Anti-corrosion Performance of Polymeric Epoxy Resin and their Zinc Phosphate Composite on 15CDV6 Steel in 3wt% NaCl: Experimental and Computational Studies. J Bio-Tribo Corr. 2020;6:1-9. https://doi.org/10.1007/s40735-020-00407-1
[38] Dagdag O, Hsissou R, El Harfi A et al. Fabrication of polymer based epoxy resin as effective anti-corrosive coating for steel: computational modeling reinforced experimental studies. Surf Interf. 2020;18:100454. https://doi.org/10.1016/j.surfin.2020.100454
[39] Dagdag O, Hsissou R, Berisha A et al. Polymeric-based epoxy cured with a polyaminoamide as an anticorrosive coating for aluminum 2024-T3 surface: experimental studies supported by computational modeling. J Bio-Tribo Corr. 2019;5:1-13. https://doi.org/10.1007/s40735-019-0251-7

[40] Dagdag O, Safi Z, Hsissou R et al. Epoxy pre-polymers as new and effective materials for corrosion inhibition of carbon steel in acidic medium: Computational and experimental studies. Sci Rep. 2019;9:1-14. https://doi.org/10.1038/s41598-019-48284-0

[41] Lalami AEO, Boukhris S, Habbadi N et al. Direct one step preparation for quinazolines derivatives. Moroc J Heterocyc Chem. 2002;(1)1:37-43.

[42] Becke AD. A new mixing of Hartree–Fock and local density-functional theories. J Chem Phys. 1993;98:1372-1377. https://doi.org/10.1063/1.464304

[43] Lee C, Yang W, Parr RG. Development of the Colle-Salvetti correlation-energy formula into a functional of the electron density. Phys Rev B. 1988;37:785.

[44] Saha SK, Hens A, Chowdhury AR et al. Molecular dynamics and density functional theory study on corrosion inhibitory action of three substituted pyrazine derivatives on steel surface. Can Chem Trans. 2014;2:489-503. https://doi:10.13179/canchemtrans.2014.02.04.0137

[45] Hsissou R, Benhiba F, Abbout S. Trifunctional epoxy polymer as corrosion inhibition material for carbon steel in 1.0 M HCl: MD simulations, DFT and complexation computations. Inorg Chem Com. 2020;115:107858. https://doi.org/10.1016/j.inoche.2020.107858

[46] Hsissou R, Abbout S, Seghiri R et al. Evaluation of corrosion inhibition performance of phosphorus polymer for carbon steel in 1 M HCl: Computational studies (DFT, MC and MD simulations). J Mat Res Technol. 2020;9:2691-2703. https://doi.org/10.1016/j.jmrt.2020.01.002

[47] Saha SK, Ghosh P, Hens A et al. Density functional theory and molecular dynamics simulation study on corrosion inhibition performance of mild steel by mercapto-quinoline Schiff base corrosion inhibitor. Phys E: Low-Dimen Syst Nanostruc. 2015;66:332-341. https://doi.org/10.1016/j.physe.2014.10.035

[48] Chermette H. Chemical reactivity indexes in density functional theory. J Comput Chem. 1999;20:129-154. https://doi.org/10.1002/(SICI)1096-987X(19990115)

[49] Parr RG, Pearson RG. Absolute hardness: companion parameter to absolute electronegativity. J Amer Chem Soc. 1983;105:7512-7516. https://doi.org/10.1021/ja00364a005

[50] Pearson RG. Absolute electronegativity and hardness correlated with molecular orbital theory. Proceed Nat Academ Sci. 1986;83:8440-8441. https://doi.org/10.1073/pnas.83.22.8440

[51] Ma H, Cheng X, Li G et al. The influence of hydrogen sulfide on corrosion of iron under different conditions. Corr Sci. 2000;42:1669-1683. https://doi.org/10.1016/S0010-938X(00)00003-2

[52] Popova A, Christov M, Vasilev A. Inhibitive properties of quaternary ammonium bromides of N-containing heterocycles on acid mild steel corrosion. Part II: EIS results. Corr Sci. 2017;49:3290-3302. https://doi.org/10.1016/j.corsci.2007.03.012

[53] Molhi A, Hsissou R, Damej M et al. Contribution to the corrosion inhibition of C38 steel in 1 M hydrochloric acid medium by a new epoxy resin PGEPPP. Int J Corr Scale Inhib. 2021;10:399-418. https://doi:10.17675/2305-6894-2021-10-1-23

[54] Molhi A, Hsissou R, Damej M et al. Performance of two epoxy resins against corrosion of C38 steel in 1 M HCl: Electrochemical, thermodynamic and theoretical assessment. Int J Corr Scale Inhib. 2021;10:812-837. https://doi:10.17675/2305-6894-2021-10-2-21

[55] Oguzie E, Li Y, Wang F. Effect of 2-amino-3-mercaptopropanoic acid (cysteine) on the corrosion behaviour of low carbon steel in sulphuric acid. Electrochim Acta. 2007;53:909-914. https://doi.org/10.1016/j.electacta.2007.07.076

[56] Ansari K, Quraishi M, Singh A. Schiff's base of pyridyl substituted triazoles as new and effective corrosion inhibitors for mild steel in hydrochloric acid solution. Corr Sci. 2014;79:5-15. https://doi.org/10.1016/j.corsci.2013.10.009

[57] Yadav DK, Quraishi M, Maiti B. Inhibition effect of some benzylidenes on mild steel in 1 M HCl: an experimental and theoretical correlation. Corr Sci. 2012;55:254-266. https://doi.org/10.1016/j.corsci.2011.10.030

[58] Aljourani J, Raeissi K, Golozar M. Benzimidazole and its derivatives as corrosion inhibitors for mild steel in 1 M HCl solution. Corr Sci. 2009;51:1836-1843. https://doi.org/10.1016/j.corsci.2009.05.011

[59] Prabhu R, Venkatesha T, Shanbhag A et al. Inhibition effects of some Schiff's bases on the corrosion of mild steel in hydrochloric acid solution. Corr Sci. 2008;50:3356-3362. https://doi.org/10.1016/j.corsci.2008.09.009

[60] Hsissou R, El Harfi A. Application of Pentaglycidyl ether Penta-ethoxy Phosphorus Composites Polymers Formulated by Two Additives, Trisodium Phosphate (TSP) and Natural Phosphate (NP) and their Combination in the Behavior of the Coating on E24 Carbon Steel in NaCl 3. 5%. Analyt Bioanalyt Electrochem. 2018;10:728-738.

[61] Mu GN, Li X, Li F. Synergistic inhibition between o-phenanthroline and chloride ion on cold rolled steel corrosion in phosphoric acid. Mat Chem Phys. 2004;86:59-68. https://doi.org/10.1016/j.matchemphys.2004.01.041

[62] Hsissou R, Benzidia B, Rehioui M et al. Anticorrosive property of hexafunctional epoxy polymer HGTMDAE for E24 carbon steel corrosion in 1.0 M HCl: gravimetric, electrochemical, surface morphology and molecular dynamic simulations. Polym Bull. 2020;77:3577-3601. https://doi.org/10.1007/s00289-019-02934-5

[63] Ahamad I, Prasad R, Quraishi M. Adsorption and inhibitive properties of some new Mannich bases of Isatin derivatives on corrosion of mild steel in acidic media. Corr Sci. 2010;52:1472-1481. https://doi.org/10.1016/j.corsci.2010.01.015

[64] Naderi E, Jafari A, Ehteshamzadeh M et al. Effect of carbon steel microstructures and molecular structure of two new Schiff base compounds on inhibition performance in 1 M HCl solution by EIS. Mat Chem Phys. 2009;115:852-858. https://doi.org/10.1016/j.matchemphys.2009.03.002

[65] Singh AK, Quraishi M. Investigation of the effect of disulfiram on corrosion of mild steel in hydrochloric acid solution. Corr Sci. 2011;53:1288-1297. https://doi.org/10.1016/j.corsci.2011.01.002

[66] Wazzan N, Obot IB, Fagieh TM. The role of some triazoles on the corrosion inhibition of C1020 steel and copper in a desalination descaling solution. Desalination. 2022;527:115551. https://doi.org/10.1016/j.desal.2022.115551

[67] Hsissou R, Benhiba F, Khudhair M et al. Investigation and comparative study of the quantum molecular descriptors derived from the theoretical modeling and Monte Carlo simulation of two new macromolecular polyepoxide architectures TGEEBA and HGEMDA. J King Saud Univ Sci. 2020;32:667-676. https://doi.org/10.1016/j.jksus.2018.10.008

[68] Yıldız R. An electrochemical and theoretical evaluation of 4, 6-diamino-2-pyrimidinethiol as a corrosion inhibitor for mild steel in HCl solutions. Corr Sci. 2015;90:544-553. https://doi.org/10.1016/j.corsci.2014.10.047

[69] Kadiri L, Ouass A, Hsissou R et al. Adsorption properties of coriander seeds: Spectroscopic kinetic thermodynamic and computational approaches. J Mol Liq. 2021;343:116971. https://doi.org/10.1016/j.molliq.2021.116971

[70] Damej M, Hsissou R, Berisha A et al. New epoxy resin as a corrosion inhibitor for the protection of carbon steel C38 in 1 M HCl. Experimental and theoretical studies (DFT, MC, and MD). J Mol Struc. 2022;1254:132425. https://doi.org/10.1016/j.molstruc.2022.132425

[71] Awad MK, Mustafa MR, Elnga MMA. Computational simulation of the molecular structure of some triazoles as inhibitors for the corrosion of metal surface. J Mol Struc: Theochem. 2010;959:66-74. https://doi.org/10.1016/j.theochem.2010.08.008

[72] Herrag L, Hammouti B, Elkadiri S et al. Adsorption properties and inhibition of mild steel corrosion in hydrochloric solution by some newly synthesized diamine derivatives: experimental and theoretical investigations. Corr Sci. 2010;52:3042-3051. https://doi.org/10.1016/j.corsci.2010.05.024

[73] Benhiba F, Hsissou R, Abderrahim K et al. Development of New Pyrimidine Derivative Inhibitor for Mild Steel Corrosion in Acid Medium. J Bio-Tribo Corr. 2022;8:36. https://doi.org/10.1007/s40735-022-00637-5

[74] Abbout S, Hsissou R, Erramli H et al. Gravimetric, electrochemical and theoretical study, and surface analysis of novel epoxy resin as corrosion inhibitor of carbon steel in 0.5 M H_2SO_4 solution. J Mol Struc. 2021;1245:131014. https://doi.org/10.1016/j.molstruc.2021.131014

[75] Abbout S, Hsissou R, Chebabe D et al. Investigation of the anti-corrosion properties of Galactomannan as additive in epoxy coatings for carbon steel: Rheological and electrochemical study. Inorg Chem Commun. 2021;134:108971. https://doi.org/10.1016/j.inoche.2021.108971

[76] Lebrini M, Lagrenée M, Traisnel M et al. Enhanced corrosion resistance of mild steel in normal sulfuric acid medium by 2, 5-bis (n-thienyl)-1, 3, 4-thiadiazoles: electrochemical, X-ray photoelectron spectroscopy and theoretical studies. Appl Surf Sci. 2007;253:9267-9276. https://doi.org/10.1016/j.apsusc.2007.05.062

[77] Hsissou R, Benhiba F, Zarrouk A et al. Electrochemical studies, Monte Carlo simulation and DFT of a new composite - pentaglycidyl ether pentaphenoxy of phosphorus - crosslinked and hybrid in its coating behavior on E24 carbon steel in 3.5% NaCl. Port Electrochim Acta. 2021;39:1-19. https://doi:10.4152/pea.202101001